

A.H. TAQI, M.A. HASAN

Department of Physics, College of Science, Kirkuk University  
(Kirkuk, Iraq; e-mail: Alitaqi@uokirkuk.edu.iq)

## SKYRME–HARTREE–FOCK–BOGOLIUBOV CALCULATIONS OF EVEN AND ODD NEUTRON-RICH Mg ISOTOPES

Using the Skyrme functional with SIII, SKM\*, SLy4, and UNE0 sets of parameters and the Hartree–Fock–Bogoliubov mean-field method; the ground-state properties of even-even and even-odd neutron-rich Mg isotopes have been investigated. The results of calculations of the binding energy per nucleon ( $B/A$ ), the one- and two-neutron separation energies ( $S_n$  and  $S_{2n}$ ), proton and neutron rms radii, neutron pairing gap, and quadrupole deformation parameter ( $\beta_2$ ) have been compared with the available experimental data, the results of Hartree–Fock–Bogoliubov calculations based on the D1S Gogny force, and predictions of some nuclear models such as the Finite Range Droplet Model (FRDM) and Relativistic Mean-Field (RMF) model. Our results show good agreements in comparison with the experimental data and the results of the mentioned models.

**Keywords:** Hartree–Fock–Bogoliubov theory, Mg isotopes, binding energy, proton and neutron rms radii, quadrupole deformation parameter ( $\beta_2$ ).

### 1. Introduction

In the theoretical nuclear physics, when we deal with a system which consists of many particles, a lot of challenges appear. One of the great challenges is to explain the nuclear structure in terms of the nucleons. It is necessary to understand the mutual interaction between those nucleons and to find a suitable solution of the equations of the corresponding many-body problem [1]. The theoretical and experimental studies of the ground-state properties (such as exotic nuclei, large deformations, high spins, ... *etc.*) of unstable and unusual nuclei (especially, for the exotic nuclei that are far from the line of  $\beta$ -stability toward the neutron-drip line) represent a very promising research domain for nuclear physics. Moreover, the experimental masses (binding energies) near the neutron-drip line are unknown [2–5]. As moving toward the neutron-drip line, some neutron-rich nuclei tend to be deformed nuclei and are often called nuclei in the “island of inversion” [6].

One of the main aspects of research in the nuclear structure physics is the development of a unified theoretical framework aimed to make reliable predictions within one nuclear model in order to de-

scribe the ground-state properties of all even and odd- $A$  nuclei. Such a microscopic description of nuclei provides many advantages, even for the most exotic nuclei and nuclear states unreachable experimentally [1, 7]. One of the most important nuclear theories that are widely used in calculations is the Hartree–Fock–Bogoliubov (HFB) approach [8–14], which unifies the self-consistent mean-field description of nuclear orbitals, as given by the Hartree–Fock (HF) theory, and the pairing correlations, as given by the Bardeen–Cooper–Schrieffer (BCS) theory of superconductivity in metals [15] into a single variational theory [9].

Magnesium (Mg,  $Z = 12$ ), as well as all the nuclei which have neutron numbers close to the magic number  $N = 20$  or  $N = 28$  (which is known as the “island of inversion”), possesses many interesting nuclear properties. There are many studies of the properties of magnesium isotopes. In particular, the ground-state properties of neutron-rich Mg isotopes were considered within the Folding model, Antisymmetrized Molecular Dynamics (AMD), modified Woods–Saxon, spherical HF, and HFB models [16], and the modified HF+BCS method with the use of SLy4, SGII, and Sk3 sets of parameters [17]. In this paper, we will be interested in calculating and analyz-

ing some nuclear ground-state properties of even-even and even-odd neutron-rich Mg isotopes over a wide collection of isotopes (from  $N = 8$  to  $N = 47$ ) in the framework of the Skyrme–Hartree–Fock–Bogoliubov (SHFB) method. We will use four well-established sets of Skyrme parameters: SIII, SKM\*, SLy4, and UNE0. The calculated properties of Mg isotopes include the binding energy per nucleon ( $B/A$ ), one- and two-neutron separation energies ( $S_n$  and  $S_{2n}$ ), proton and neutron rms radii, neutron pairing gap, quadrupole deformation parameter ( $\beta_2$ ), and potential energy curves and will be compared with the available experimental data of the Atomic Mass Evaluation (AME2016) [18] and with the results of different models such as the Finite Range Droplet Model (FRDM) [19], Relativistic Mean-Field (RMF) model [20], and HFB calculations based on the D1S Gogny force [21].

## 2. Hartree–Fock–Bogoliubov Theory

In the Hartree–Fock–Bogoliubov formalism, a two-body Hamiltonian of a system of fermions can be expressed in terms of a standard set of annihilation and creation operators ( $c, c^\dagger$ ) [10]:

$$H = \sum_{k_1 k_2} e_{k_1 k_2} c_{k_1}^\dagger c_{k_2} + \frac{1}{4} \sum_{k_1 k_2 k_3 k_4} \bar{v}_{k_1 k_2 k_3 k_4} c_{k_1}^\dagger c_{k_2}^\dagger c_{k_4} c_{k_3}. \quad (1)$$

where the first term corresponds to the kinetic energy, and  $\bar{v}_{k_1 k_2 k_3 k_4} = \langle k_1 k_2 | V | k_3 k_4 - k_4 k_3 \rangle$  is the matrix element of the two-body interaction between antisymmetrized two-particle states. The HFB ground-state wave function  $|\Phi\rangle$  is defined as the quasiparticle vacuum  $\alpha_k |\Phi\rangle = 0$ , where the quasiparticle operators ( $\alpha, \alpha^\dagger$ ) are connected to the original particle operators via a linear Bogoliubov transformation [10]:

$$\alpha_k = \sum_{\dot{k}} (U_{\dot{k}k}^* c_{\dot{k}} + V_{\dot{k}k}^* c_{\dot{k}}^\dagger), \alpha_k^\dagger = \sum_{\dot{k}} (V_{\dot{k}k} c_{\dot{k}} + U_{\dot{k}k} c_{\dot{k}}^\dagger). \quad (2)$$

which can be rewritten in the matrix form as

$$\begin{pmatrix} \alpha \\ \alpha^\dagger \end{pmatrix} = \begin{pmatrix} U^\dagger & V^\dagger \\ V^T & U^T \end{pmatrix} \begin{pmatrix} c \\ c^\dagger \end{pmatrix}. \quad (3)$$

The matrices  $U$  and  $V$  satisfy the relations [10]

$$\left. \begin{aligned} U^\dagger U + V^\dagger V &= I, \\ U U^\dagger + V^* V^T &= I, \\ U^T V + V^T U &= 0, \\ U V^\dagger + V^* U^T &= 0. \end{aligned} \right\} \quad (4)$$

In terms of the normal density  $\rho$  and pairing tensor  $\kappa$ , the one-body density matrices are:

$$\left. \begin{aligned} \rho_{k\dot{k}} &= \langle \Phi | c_{\dot{k}}^\dagger c_k | \Phi \rangle = (V^* V^T)_{k\dot{k}}, \\ \kappa_{k\dot{k}} &= \langle \Phi | c_{\dot{k}} c_k | \Phi \rangle = (V^* U^T)_{k\dot{k}}. \end{aligned} \right\} \quad (5)$$

The expectation value of Eq. (1) can be expressed in an energy functional as [10]

$$E[\rho, \kappa] = \frac{\langle \Phi | H | \Phi \rangle}{\langle \Phi | \Phi \rangle} = \text{Tr} \left[ \left( e + \frac{1}{2} \Gamma \right) \rho \right] - \frac{1}{2} \text{Tr} [\Delta \kappa^*], \quad (6)$$

where the self-consistent term is

$$\Gamma_{k_1 k_3} = \sum_{k_2 k_4} \bar{v}_{k_1 k_2 k_3 k_4} \rho_{k_4 k_2}, \quad (7)$$

and the pairing field term is

$$\Delta_{k_1 k_2} = \frac{1}{2} \sum_{k_3 k_4} \bar{v}_{k_1 k_2 k_3 k_4} \kappa_{k_3 k_4}. \quad (8)$$

The variation of the energy [Eq. (6)] with respect to  $\rho$  and  $\kappa$  leads to the HFB equations [10]

$$\begin{pmatrix} e + \Gamma - \lambda & \Delta \\ -\Delta^* & -(e + \Gamma)^* + \lambda \end{pmatrix} \begin{pmatrix} U \\ V \end{pmatrix} = E \begin{pmatrix} U \\ V \end{pmatrix}. \quad (9)$$

where  $\lambda$  is the Lagrange multiplier used to fix the correct average particle number, and  $\Delta$  refers to the pairing potential. More details about the HFB theory and Skyrme HFB equations can be found in Refs [10, 11].

## 3. Details of Calculations

In this work, the ground-state properties of even-even and even-odd neutron-rich Mg isotopes have been reproduced by using the HFBTHO code (v2.00d) [11]. The code iteratively diagonalizes the Hamiltonian based on the Skyrme functional until a self-consistent solution is achieved. More details can be found in Refs. [10, 11].

Calculations were performed with the Skyrme functional for SIII [22], SKM\* [23], SLy4 [24], and UNE0 [25] sets of parameters. A mixed volume-surface pairing force has been used with a cutoff quasiparticle energy  $E_{\text{cut}} = 60$  MeV. The harmonic oscillator (HO) basis was characterized by the oscillator length  $b = -1.0$  fm, which means that the code automatically sets  $b_0$  by using the relation of HO frequency [11]:

$$b_0 = \sqrt{\hbar/m\omega}, \quad (10)$$

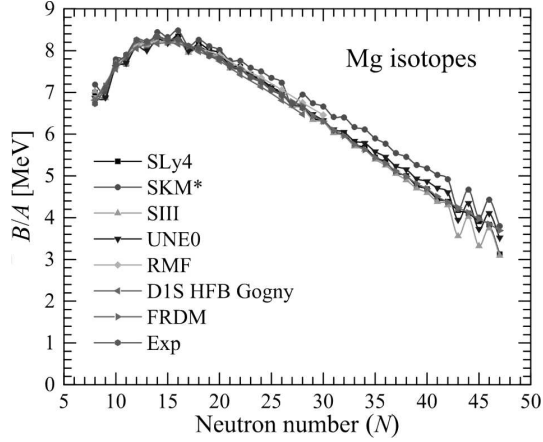


**Fig. 1.** HFBTHO calculations of the  $B/A$  for even-even and even-odd Mg isotopes by using SIII, SKM\*, SLy4, and UNE0 forces

where  $\hbar\omega = 1.2 \times 41/A^{1/3}$ . The number of oscillator shells (the principal number of oscillator shells  $N$ ) taken into account was  $N_{\max} = 20$  shells [10, 11]. The input data on the pairing strength in HFBTHO program [11] in Eq. (11) for neutrons  $V_0^n$  and protons  $V_0^p$  (in MeV) have been used as a pre-defined pairing force depending on a standard value of each Skyrme functional that is used in the HFBTHO program,

$$V_{pair}^{n,p}(\mathbf{r}) = V_0^{n,p} \left(1 - \alpha \frac{\rho(\mathbf{r})}{\rho_c}\right) \delta(\mathbf{r} - \hat{\mathbf{r}}), \quad (11)$$

where  $\rho(\mathbf{r})$  is the local density, and  $\rho_c$  is the saturation density fixed at  $\rho_c = 0.16 \text{ fm}^{-3}$ , and the type of pairing force is defined by the parameter  $\alpha$ , which can be a volume, surface, or mixed volume-surface char-

**Table 1. Skyrme sets of parameters that have been used in this work**

Parameters	SIII [22]	SKM* [23]	SLy4 [24]	UNE0 [25]
$t_0$ (MeV · fm <sup>3</sup> )	-1128.75	-2645.0	-2488.9	-1883.6
$t_1$ (MeV · fm <sup>5</sup> )	395.0	410.0	486.8	277.5
$t_2$ (MeV · fm <sup>5</sup> )	-95.0	-135.0	-546.3	608.4
$t_3$ (MeV · fm <sup>5</sup> )	14000.0	15595.0	13777.0	13901.9
$x_0$	0.45	0.090	0.834	0.974
$x_1$	0.0	0.0	-0.344	-1.777
$x_2$	0.0	0.0	-1.0	-1.676
$x_3$	1.0	0.0	1.345	-0.380
$W_0$ (MeV · fm <sup>3+3σ</sup> )	120.0	130.0	123.0	0.0
$\sigma$	1.00	1/6	1/6	1/3.11

acteristic [11]. The different sets of parameters of the Skyrme forces used in this study are shown in Table 1.

## 4. Results and Discussion

In this section, we present the numerical results for the ground-state properties of the even-even and even-odd Mg isotopes which have been investigated in the framework of the HFB method.

### 4.1. Binding Energy

The results of HFBTHO calculations of the binding energies per nucleon ( $B/A$ ) as a function of the neutron number ( $N$ ) are depicted in Fig. 1 and are compared with the available experimental data of AME2016 [18], the data of Finite Range Droplet Model (FRDM) [19], the results of Relativistic Mean-Field (RMF) model [20], and the data of HFB calculations based on the D1S Gogny force [21]. As shown in Fig. 1, the calculated binding energies are consistent with the experimental data and with the results of the mentioned models, except some nuclei ( $N = 43 \rightarrow 47$ ) which show fluctuations in their energy in all the interactions used, except the SLy4 force. In the last case, we see a fluctuation in the binding energy only for  $N = 47$ .

The difference between the calculated  $B/A$  and the results of FRDM [19], RMF [20], and D1S-Gogny HFB [21] are presented in Fig. 2. The comparisons are made only for isotopes for which the experimental data are available. The differences were very close for the most of the isotopic chain, but some differences ( $\leq \pm 0.45$  MeV) were found for the light nuclei, exactly in the region with  $N = 8$ . For the region with  $N = 26$  and 28 with the SKM\* force, the differences was 0.3 MeV.

### 4.2. One- and Two-Neutron Separation Energy

The one- ( $S_n$ ) and two-neutron ( $S_{2n}$ ) separation energies for even-even and even-odd Mg isotopes have been calculated by using HFBTHO code [11] with Skyrme-SIII, SKM\*, SLy4, and UNE0 sets of parameters. The single-neutron separation energy is defined as

$$S_n(Z, N) = B(Z, N) - B(Z, N - 1), \quad (12)$$

and the double-neutron separation energy is as follows:

$$S_{2n}(Z, N) = B(Z, N) - B(Z, N - 2). \quad (13)$$

The calculated results of  $S_n$  for Mg isotopes with SIII, SKM\*, SLy, and UNE0 interactions can be found in Fig. 3. They have been compared with the available data of AME2016 [18] and the data of FRDM [19]. The  $S_n$  starts with a large value in the light nuclei region; then it begins to decrease, as the number of neutrons increases. From this figure, it is seen that  $S_n$  of even nuclei is greater than their odd neighbors. From Fig. 3, it can be seen that the results for the SLy4 force are more consistent with the experimental data and with the results of FRDM than those of other forces used.

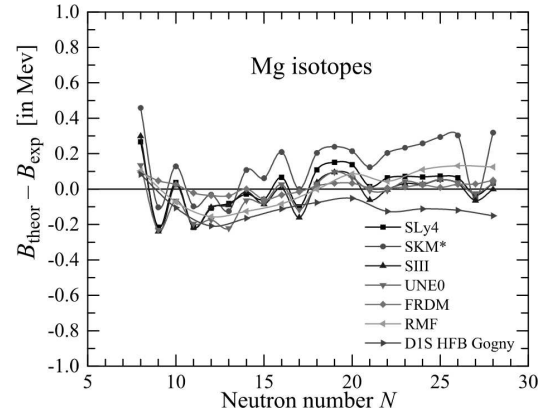
Figure 4 shows the calculated  $S_{2n}$  for even-even and even-odd Mg isotopes as functions of the neutron number  $N$ ; they are obtained with Skyrme SIII, SKM\*, SLy4, and UNE0 forces. The calculated results of  $S_{2n}$  have been compared with the available experimental data of AME2016 [18], FRDM data [19], the results of RMF [20], and the data of D1S Gogny-HFB [21]. It can be seen from Fig. 4 that the results for the SLy4 force are the most consistent and the closest to the experimental data and to the other models' results.

### 4.3. Quadrupole deformation

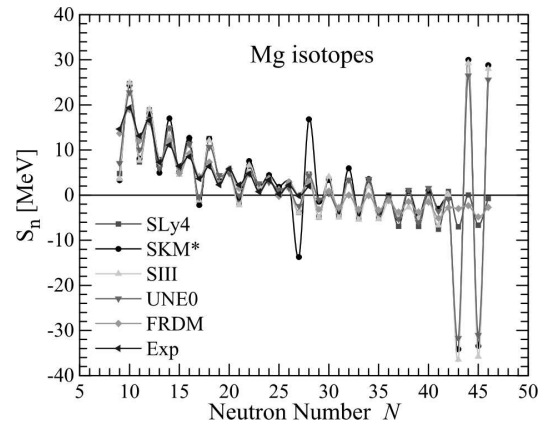
An important information about nuclear properties can be obtained from the calculations of quadrupole deformation parameter ( $\beta_2$ ) such as the size, quadrupole moment, and shape of the nucleus (spherical or deformed) [26].

Figure 5 presents the HFBTHO calculations of the quadrupole deformation parameter ( $\beta_2$ ) by using Skyrme SIII, SKM\*, SLy4, and UNE0 forces for even and odd Mg isotopes as functions of the neutron number ( $N$ ) in comparison with the available experimental data [27], FRDM data [19], RMF data [20], and the results of D1S-Gogny HFB [21].

From Fig. 5, the closed shells with the magic numbers  $N = 8$  and  $N = 20$  have  $\beta_2 = 0$ , as expected, which corresponds to spherical nuclei. Nuclei which are above  $N = 8$  and  $N = 20$  show an interesting change in their shape. The deformed or prolate shape has maximum  $\beta_2 \approx 0.44$  at  $N = 11$  and  $\beta_2 \approx 0.39$  at  $N = 27$  for all interactions. Above  $N = 28$ , there is a transition from a deformed to spherical shape; especially for even nuclei which have  $\beta_2 \approx 0$ . The strong deformation appears in the region within  $8 \leq N \leq 14$ ,  $22 \leq N \leq 32$ , and from  $N = 39$  to  $N = 47$  for



**Fig. 2.** The difference between the calculated  $B/A$  and the results of FRDM [19], RMF [20], and D1S-Gogny HFB [21]



**Fig. 3.** Results of HFBTHO calculations of  $S_n$  for even-even and even-odd Mg isotopes in comparison with the experimental data [18] and the data of FRDM model [19]

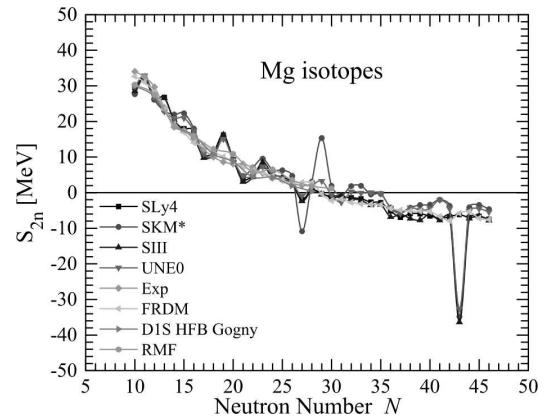


**Fig. 4.** Results of HFBTHO calculations of  $S_{2n}$  for even-even and even-odd Mg isotopes in comparison with the experimental data [18], the data of FRDM model [19], the results of RMF model [20], and the data of D1S-Gogny HFB model [21]

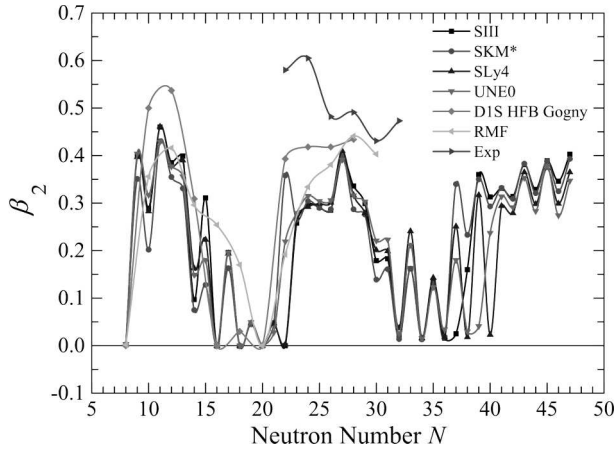


**Fig. 5.** Results of HFBTHO calculations of the quadrupole deformation parameter ( $\beta_2$ ) for even-even and even-odd Mg isotopes in comparison with the experimental data [27], FRDM data [19], RMF data [20], and the results of D1S-Gogny HFB [21]

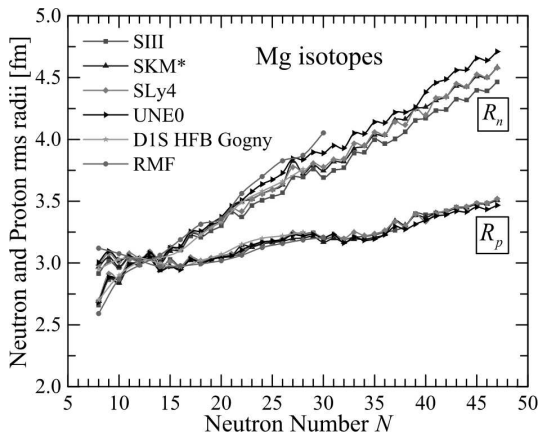


**Fig. 6.** Results of HFBTHO calculations of  $R_n$  and  $R_p$  for even-even and even-odd Mg isotopes in comparison with RMF data [20] and D1S-Gogny HFB calculations [21]

the isotopic chain. From the comparison between the HFBTHO calculations and other results, very good agreements were obtained, as it is clearly seen in Fig. 5.

#### 4.4. Neutron and proton rms radii

The HFBTHO calculations of the neutron and proton rms radii ( $R_n$  and  $R_p$ ) for even-even and even-odd Mg isotopes are plotted as functions of the neutron number  $N$  in Fig. 6 with Skyrme: SIII, SKM\*, SLy4, and UNE0 interactions. The results of HFBTHO calculations of the neutron and proton rms radii have been

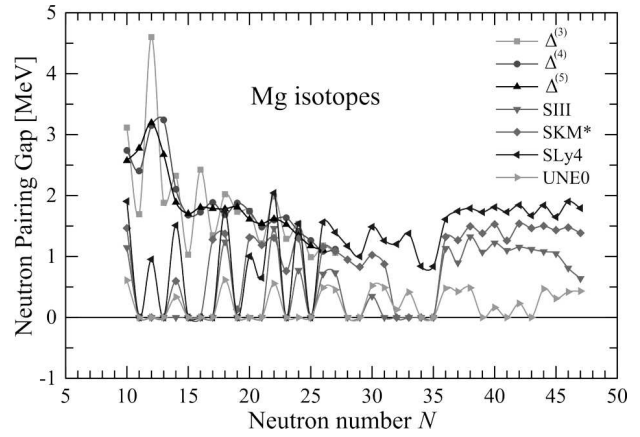


**Fig. 7.** Results of HFBTHO calculations of the neutron pairing gap for even-even and even-odd Mg isotopes in comparison with difference formulas  $\Delta^{(3)}$ ,  $\Delta^{(4)}$  and  $\Delta^{(5)}$  of the experimental data of AME2016 [18]

compared with the available results of RMF [20] and the results of D1S-Gogny HFB calculations [21] and are shown in Fig. 6 for comparison. The calculated results of  $R_n$  and  $R_p$  have been plotted together in order to see the differences between them.

From Fig. 6, it is seen that the differences between  $R_n$  and  $R_p$  start to increase with  $N$ . This difference reaches at 1.244 fm for  $^{59}\text{Mg}$  with Skyrme-UNE0 force, 0.945 fm with Skyrme-SIII, and 1.06 fm with Skyrme-SKM\* and SLy4 forces simultaneously. Near the  $\beta$ -stability line (when  $N \approx Z$ ),  $R_n$  and  $R_p$  are almost the same for all the examined interactions. The calculated results with Skyrme SIII, SKM\*, SLy4, and UNE0 interactions show a good agreement with available data of RMF and the results of D1S-Gogny HFB, especially in the region  $8 \leq N \leq 20$ .

#### 4.5. Neutron pairing gap

The results of HFBTHO calculations of the neutrons pairing gap as a function of the neutron number  $N$  are shown in Fig. 7. The results are compared with many finite-difference formulas, which are often interpreted as a measurement of the empirical pairing gap of three-point  $\Delta_Z^{(3)}$ , four-point  $\Delta_Z^{(4)}$ , and five-point  $\Delta_Z^{(5)}$  difference formulas [26, 28, 29]. The three-point  $\Delta_Z^{(3)}$  difference formula can be written as [30]:

$$\Delta_Z^{(3)}(N) \equiv \frac{\pi N}{2} [B(Z, N-1) + B(Z, N+1) - 2B(Z, N)], \quad (14)$$

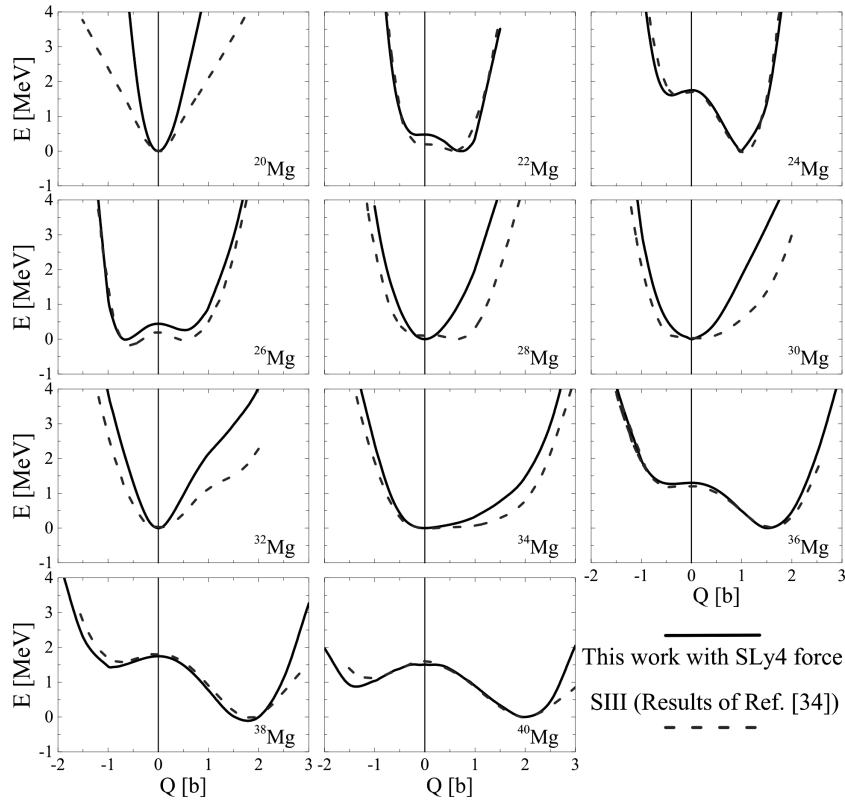


**Fig. 8.** Results of HFBTHO calculations of the deformation energy curves by using the Skyrme SLy4 force for even-even  $^{20\rightarrow 40}\text{Mg}$  isotopes in comparison with the results of Ref. [34] as a function of the axial quadrupole moment. The origin of the energy is taken at the minimum of each curve

the four-point  $\Delta_Z^{(4)}$  difference formula can be defined as [31–33]:

$$\Delta_Z^{(4)}(N) \equiv \frac{\pi_N}{4} [B(Z, N - 2) - 3B(Z, N - 1) - B(Z, N + 1) + 3B(Z, N)], \quad (15)$$

and the five-point  $\Delta_Z^{(5)}$  difference formulas can be defined as [29]:

$$\Delta_Z^{(5)}(N) \equiv -\frac{\pi_N}{8} [B(Z, N + 2) + 6B(Z, N) + B(Z, N - 2) - 4B(Z, N + 1) - 4B(Z, N - 1)]. \quad (16)$$

Here,  $\pi_N = (-1)^N$  is the number parity,  $B$  is the experimental binding energy values given in Ref. [18], and  $Z$  and  $N$  are the proton and neutron numbers, respectively.

The neutron pairing gaps (effective gap) of HFBTHO code is defined as the mean value of the pairing field  $\Delta$  [10, 26]:

$$\bar{\Delta} = \frac{\text{Tr} \Delta \rho}{\text{Tr} \rho}, \quad (17)$$

where  $\rho$  refers to the normal one-body density matrix. This may be one of the reasons for the difference between HFBTHO calculations and the results of experimental data. The calculated pairing gaps are exactly zero for closed shell (magic number) nuclei at  $N = 20$ , as is clearly seen in Fig. 7 for SIII and UNE0 interactions. When  $\Delta$  becomes zero,  $\bar{\Delta}$  vanishes, which corresponds to the maximum values of the gaps given by the empirical formulas. Another remark that can be seen in Fig. 7 is that the even nuclei have larger pairing gaps than that of odd nuclei for all the examined interactions, and, especially, for Skyrme SLy4 set. This occurs, because the block-

ing of one state in the odd nuclei does not contribute to the pairing potential, leading to overall smaller single particle gaps [26, 29]. It is seen from Fig. 7 that the result with SLy4 force is the closest to the finite-difference formulas of neutron pairing gaps than the results with other examined Skyrme forces.

#### 4.6. Potential energy curves

Based on the calculated results of the  $B$ ,  $S_n$ ,  $S_{2n}$ , and neutron pairing gap with the SLy4 force which showed a good agreement with the experimental results, we calculated the potential energy curves of the investigated even-even  $^{20\rightarrow 40}\text{Mg}$  isotopes with the SLy4 force and plotted them as functions of their axial quadrupole moment  $Q(b)$  in Fig. 8. The well-defined spherical shape was obtained for  $^{22\rightarrow 24}\text{Mg}$  isotopes. All deformed isotopes of Mg turn out prolate with the exception of  $^{26}\text{Mg}$ . The potential energy curve of  $^{32}\text{Mg}$  has well-defined prolate minima and shows an inflection point at the axial quadrupole moment  $Q = 1.5b$ . A very shallow oblate minimum appears roughly at an energy of 1.0 MeV for  $^{36}\text{Mg}$ ,  $^{38}\text{Mg}$ , and  $^{40}\text{Mg}$  isotopes. In general, we found the excellent similarity between the HFBTHO calculations with Skyrme SLy4 force and the previously published results of Ref. [34], especially in heavy Mg isotopes which have neutron number  $N = 24, 26$  and  $28$  as seen in Fig. 8.

#### 5. Conclusions

In this paper, the ground-state properties of even-even and even-odd Mg isotopes have been investigated using HFB approach with the Skyrme sets SIII, SKM\*, SLy4 and UNE0. The studied properties including the binding energy per nucleon ( $B/A$ ), one- and two-neutron separation energies ( $S_n, S_{2n}$ ), proton and neutron rms radii, neutron pairing gap, quadrupole deformation parameter ( $\beta_2$ ), and potential energy curves which have been compared with the available experimental data, the results of HFB calculations based on the D1S Gogny effective nucleon-nucleon interaction, and predictions of some nuclear models such as the Finite Range Droplet Model (FRDM) and Relativistic Mean-Field (RMF) model. The calculated results with different Skyrme functional parameters (especially with the Skyrme SLy4 force) show a very good agreement and are consistent with the available experimental data and

the results of other models. The differences between light and heavy nuclei are clear; in addition, the effect of increasing number of neutrons on the ground-state properties can be seen in the presented figures; this is especially true for the binding energy, neutron and proton rms radii, quadrupole deformation parameter ( $\beta_2$ ), and potential energy curves. Moreover, the calculated potential energy surface with the Skyrme SLy4 force shows a clear shape transition (from spherical shape to: prolate, oblate, and prolate-oblate shapes) for the investigated Mg isotopic chain.

1. F. Chappert, N. Pillet, M. Girod, J.-F. Berger. Gogny force with a finite-range density dependence. *Phys. Rev. C* **91**, 034312 (2015).
2. R. Rodriguez-Guzman, P. Sarriguren, L.M. Robledo, S. Perez-Martin. Charge radii and structural evolution in Sr, Zr, and Mo isotopes. *Phys. Lett. B* **691**, 202 (2010).
3. W. Nazarewicz, T. R. Werner, J. Dobaczewski. Mean-field description of ground-state properties of drip-line nuclei: Shell-correction method. *Phys. Rev. C* **50**, 2860 (1994).
4. J. Dobaczewski, W. Nazarewicz, T.R. Werner, J.F. Berger, C.R. Chinn, J. Decharge. Mean-field description of ground-state properties of drip-line nuclei: Pairing and continuum effects. *Phys. Rev. C* **53**, 2809 (1996).
5. F. Chappert, M. Girod, S. Hilaire. Towards a new Gogny force parametrization: Impact of the neutron matter equation of state. *Phys. Lett. B* **668**, 420 (2008).
6. I. Hamamoto. Change of shell structure and magnetic moments of odd-N deformed nuclei towards the neutron drip line. *J. Phys. G: Nucl. Part. Phys.* **37**, 055102 (2010).
7. J.C. Pei, M.V. Stoitsov, G.I. Fann, W. Nazarewicz, N. Schunck, F.R. Xu. Deformed coordinate-space Hartree-Fock-Bogoliubov approach to weakly bound nuclei and large deformations. *Phys. Rev. C* **78**, 064306 (2008).
8. V.E. Oberacker, A.S. Umar, E. Teran, A. Blazkiewicz. Hartree-Fock-Bogoliubov calculations in coordinate space: Neutron-rich sulfur, zirconium, cerium, and samarium isotopes. *Phys. Rev. C* **68**, 064302 (2003).
9. P. Ring, P. Schuck. *The Nuclear Many-Body Problem* (Springer, 1980) [ISBN: 0-387-09820-8].
10. M.V. Stoitsov, J. Dobaczewski, W. Nazarewicz, P. Ring. Axially deformed solution of the Skyrme-Hartree-Fock-Bogoliubov equations using the transformed harmonic oscillator basis. The program HFBTHO (v1.66p). *Comput. Phys. Commun.* **167**, 43 (2005).
11. M.V. Stoitsov, N. Schunck, M. Kortelainen, N. Michel, H. Nam, E. Olsen, J. Sarich, S. Wild. Axially deformed solution of the Skyrme-Hartree-Fock-Bogoliubov equations using the transformed harmonic oscillator basis (II) HFBTHO v2.00d: A new version of the program. *Comput. Phys. Commun.* **184**, 1592 (2013).

12. M. Bender, P.-H. Heenen, P.-G. Reinhard. Self-consistent mean-field models for nuclear structure. *Rev. Mod. Phys.* **75**, 121 (2003).
13. J. Dobaczewski, H. Flocard, J. Treiner. Hartree-Fock-Bogolyubov description of nuclei near the neutron-Drip Line. *Nucl. Phys. A* **422**, 103 (1984).
14. A. Bulgac. Hartree–Fock–Bogoliubov approximation for finite systems. IPNE FT-194-1980, Bucharest (arXiv: nucl-th/9907088) (1980).
15. J. Bardeen, L.N. Cooper, J.R. Schrieffer. Theory of Superconductivity. *Phys. Rev.* **108**, 1175 (1957).
16. S. Watanabe, K. Minomo, M. Shimada, S. Tagami, M. Kimura, M. Takechi, M. Fukuda, D. Nishimura, T. Suzuki, T. Matsumoto, Y.R. Shimizu, M. Yahiro. Ground-state properties of neutron-rich Mg isotopes. *Phys. Rev. C* **89**, 044610 (2014).
17. M.K. Gaidarov, P. Sarriguren, A.N. Antonov, E. Moya de Guerra. Ground-state properties and symmetry energy of neutron-rich and neutron-deficient Mg isotopes. *Phys. Rev. C* **89**, 064301 (2014).
18. M. Wang, G. Audi, F.G. Kondev, W.J. Huang, S. Naimi, X. Xu. The AME2016 atomic mass evaluation (II). Tables, graphs and references. *Chin. Phys. C* **41**, 030003 (2017).
19. P. Moller, A. Sierk, T. Ichikawa, H. Sagawa. Nuclear ground-state masses and deformations: FRDM (2012). *Atom. Data Nucl. Data Tables* **109–110**, 1 (2016).
20. G.A. Lalazissis, S. Raman, P. Ring. Ground-State Properties of Even-Even Nuclei in the Relativistic Mean-Field Theory. *Atom. Data Nucl. Data Tables* **71**, 1 (1999).
21. [http://www-phynu.cea.fr/HFB-Gogny\\_eng.htm](http://www-phynu.cea.fr/HFB-Gogny_eng.htm).
22. M. Beiner, H. Flocard, N.V. Giai, P. Quentin. Nuclear ground-state properties and self-consistent calculations with the Skyrme interaction: (I). Spherical description. *Nucl. Phys. A* **238**, 29 (1975).
23. J. Bartel, P. Quentin, M. Brack, C. Guet, H.-B. Hakansson. Towards a better parametrization of Skyrme-like effective forces: A critical study of the SkM force. *Nucl. Phys. A* **386**, 79 (1982).
24. E. Chabanat, P. Bonche, P. Haensel, J. Meyer, R. Schaeffer. A Skyrme parametrization from subnuclear to neutron star densities Part II. Nuclei far from stabilities. *Nucl. Phys. A* **635** (1–2), 231 (1998).
25. M. Kortelainen, T. Lesinski, J. More, W. Nazarewicz, J. Sarich, N. Schunck, M.V. Stoitsov, S. Wild. Nuclear energy density optimization. *Phys. Rev. C* **82**, 024313 (2010).
26. Y. El Bassem, M. Oulne. Hartree–Fock–Bogoliubov calculation of ground state properties of even-even and odd Mo and Ru isotopes. *Nucl. Phys. A* **957**, 22 (2016).
27. <http://www-nds.iaea.org/RIPL-2/masses/gs-deformations-exp.dat> (30/07/2015).
28. A.H. Taqi, M.A. Hasan. Ground-state properties of even-even nuclei from He ( $Z = 2$ ) to Ds ( $Z = 110$ ) in the framework of Skyrme-Hartree–Fock–Bogoliubov theory. *Arab. J. Sci. Eng.* (2021).
29. M. Bender, K. Rutz, P.-G. Reinhard, J.A. Maruhn. Pairing gaps from nuclear mean-field models. *Eur. Phys. J. A* **8**, 59 (2000).
30. W. Satula, J. Dobaczewski, W. Nazarewicz. Odd-even staggering of nuclear masses: Pairing or shape effect?. *Phys. Rev. Lett* **81**, 3599 (1998).
31. A. Bohr, B.R. Mottelson. *Nuclear Structure Volume I: Single-Particle Motion* (Wor. Sci. publ. Co. Pte. Ltd, 1998) [ISBN: 9810239793].
32. S.J. Krieger, P. Bonche, H. Flocard, P. Quentin, M.S. Weiss. An improved pairing interaction for mean field calculations using skyrme potentials. *Nucl. Phys. A* **517**, 275 (1990).
33. S. Cwiok, J. Dobaczewski, P.-H. Heenen, P. Magierski, W. Nazarewicz. Shell structure of the superheavy elements. *Nucl. Phys. A* **611**, 211 (1996).
34. J. Terasaki, H. Flocard, P.-H. Heenen, P. Bonche. Deformation of nuclei close to the two-neutron drip line in the Mg region. *Nucl. Phys. A* **621**, 706 (1997).

Received 23.07.20

A.X. Тахі, М.А. Хасан

РОЗРАХУНКИ ПАРНИХ І НЕПАРНИХ  
ІЗОТОПІВ Mg З ВИСОКИМ ВМІСТОМ НЕЙТРОНІВ  
МЕТОДОМ ХАРТРІ–ФОКА–БОГОЛЮБОВА

Застосовуючи функціонал Скірма з наборами параметрів SIII, SKM\*, SLy4 і UNE0 та метод середнього поля Хартрі–Фока–Боголюбова, ми вивчили властивості основного стану парно-парних та парно-непарних ізотопів Mg з високим вмістом нейтронів. Результати розрахунків енергії зв'язку на нуклон ( $B/A$ ), енергій відділення одного та двох нейтронів ( $S_n$  і  $S_{2n}$ ), середньоквадратичних радіусів протона та нейтрона, величини щільності для парування нейтронів та параметра квадрупольної деформації ( $\beta_2$ ) порівнюються з наявними експериментальними даними, з результатами розрахунків у підході Хартрі–Фока–Боголюбова з використанням D1S Гогні сил та з передбаченням деяких моделей ядер, таких як крапельна модель ядра та релятивістська модель середнього поля. Отримано гарну узгодженість з експериментом та результатами згаданих моделей.

*Ключові слова:* теорія Хартрі–Фока–Боголюбова, ізотопи Mg, енергія зв'язку, середньоквадратичні радіуси протона та нейтрона, параметр квадрупольної деформації ( $\beta_2$ ).